SCIENTIFIC REPORTS

OPEN

SUBJECT AREAS:
METABOLIC DISORDERS
INFLAMMATION
OXIDOREDUCTASES

Received
21 October 2013

Accepted
16 December 2013

Published
13 January 2014

Correspondence and requests for materials should be addressed to M.A. (malemany@ub.edu)

Cultured 3T3L1 adipocytes dispose of excess medium glucose as lactate under abundant oxygen availability

David Sabater[1,2,3], Sofía Arriarán[1,2,3], María del Mar Romero[1,2,3], Silvia Agnelli[1,2,3], Xavier Remesar[1,2,3], José Antonio Fernández-López[1,2,3] & Marià Alemany[1,2,3]

[1]Department of Nutrition and Food Science, Faculty of Biology, University of Barcelona, Barcelona 08028, Spain, [2]Institute of Biomedicine, University of Barcelona, Barcelona 08028, Spain, [3]CIBER Obesity and Nutrition, Institute of Health Carlos III, Spain.

White adipose tissue (WAT) produces lactate in significant amount from circulating glucose, especially in obesity;Under normoxia, 3T3L1 cells secrete large quantities of lactate to the medium, again at the expense of glucose and proportionally to its levels. Most of the glucose was converted to lactate with only part of it being used to synthesize fat. Cultured adipocytes were largely anaerobic, but this was not a Warburg-like process. It is speculated that the massive production of lactate, is a process of defense of the adipocyte, used to dispose of excess glucose. This way, the adipocyte exports glucose carbon (and reduces the problem of excess substrate availability) to the liver, but the process may be also a mechanism of short-term control of hyperglycemia. The *in vivo* data obtained from adipose tissue of male rats agree with this interpretation.

White adipose tissue (WAT) main substrate is glucose[1,2], which uses in part to synthesize fatty acids for its triacylglycerol (TAG) stores[3]. WAT also takes up unesterified fatty acids[4] or those in lipoproteins, released by gut and liver[5,6].WAT produces lactate from glucose[7,8], in proportions that may account for up to 30% of all body glucose metabolism, as reviewed by DiGirolamo *et al.*[9]. Production of lactate is also increased in primary cultures of adipocytes from obese or diabetic humans, accounting for up to 50–70% of all glucose taken up[10], in a process dependent, at least in part, on insulin[10,11]. Lactate release by WAT has been related to obesity and insulin resistance[12], since cells from diabetic humans produce more lactate than those of healthy subjects[13]. Small adipocytes, during the process of increasing fat storage, produce less lactate from glucose than larger cells, containing more TAG[14].

WAT lactate production has been assumed to be part of a Cori cycle[15] between WAT –as peripheral organ producing lactate from glucose– and liver. The result of such large production of lactate may be an increase in liver gluconeogenesis and/or hepatic glycogen storage[16]. However, this explanation could not be quantitatively sustained under conditions of excess glucose availability, since it blocks gluconeogenesis and glycogen storage.

WAT lactate release has been often considered a telltale of hypoxia[17], correlated with acidosis[18], tissue stress[19], mitochondrial function disturbances[20], endothelial inflammation[21] and altered cytokine release pattern[22]. The paradigm of lactate release as indication of hypoxia has been challenged by direct analysis of *in vivo* oxygen levels and consumption by adipose tissue[23,24], which is relatively low. WAT blood flow is diminished in obesity[25], but the tissue could not be considered hypoxic because direct measurement of pO_2 proved that the tissue receives sufficient oxygen to sustain its metabolism given the limited needs of the tissue[24]. Low blood flow may be partly compensated by lactate release, decreasing blood pH, but freeing more oxygen from oxyhemoglobin to counter hypoxia through the Bohr effect[26]. The decrease in WAT blood flow may be a defensive mechanism, under conditions of insulin resistance, to limit the entry of blood-carried energy substrates, which the tissue has to take up as end-of-the-line dumping place[27].

Adipocyte lactate efflux in the presence of high glucose is levels may be due to:

a) a simple defense strategy to survive under hyperglycemia, limiting substrate availability to prevent unwanted hyperthrophia through decreased blood flow at the expense of lower oxygen supply. There is no hipoxia because oxygen needs may be minimized using glucose massively through anaerobic glycolysis. This may also help reduce substrate availability, or

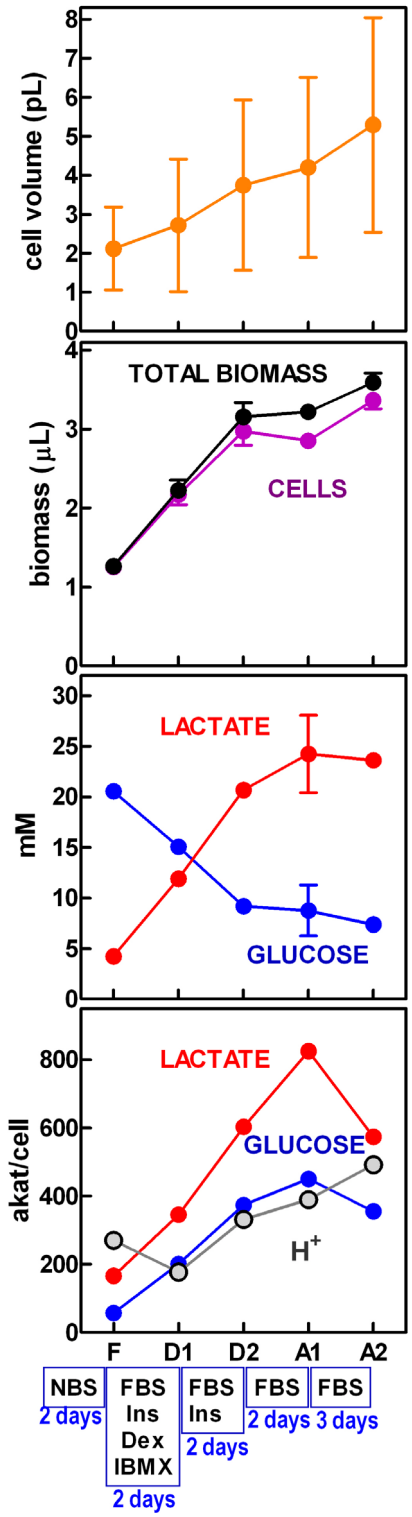

Figure 1 | Changes in cell volume, culture biomass, glucose uptake and lactate release of 3T3L1 cells along the differentiation process from fibroblasts (at confluence) to mature adipocytes. F = fibroblasts at confluence; D1 = end of the treatment with the first differentiation medium; D2 = end of the treatment with the second differentiation medium; A1 = mature adipocytes on day 6; A2 = mature adipocytes on day 9. The composition of the incubation media used in the transitions from one stage to the other are indicated at the bottom, as well as the duration of the process. NBS = neonatal bovine serum; FBS = fetal bovine serum; Ins = insulin; Dex = dexamethasone; IBMX = 3-isobutyl-1-methylxanthine, a phosphodiesterase inhibitor. The upper panel shows the mean cell volumes (±SD) for cells at the different stages of differentiation and growth in size. Since cell volume includes thousands of individual measurements we used the SD instead of SEM values to give a better idea of cell size variability The second panel shows the data for biomass (mean ± SEM) in the culture wells; purple corresponds to cells, and black to total biomass, i.e. cells and other smaller particles (largely debris formed during harvesting). The third panel shows the lactate and glucose concentrations (mean ± SEM) in the culture medium (initially lactate 0 mM, glucose 22 mM). The fourth panel presents the mean rates (in attokatals per cell) for lactate production, glucose uptake and proton release into the medium calculated (see text for information) using mean parameter values.

b) the recourse to anaerobic glycolysis is a Warburg-like[28] effect, such as that observed in fast-growing tumor cells[29]; the cells forsake oxidative phosphorylation to obtain the ATP they need by using large amounts of glucose in glycolysis to lactate[30].

In order to discern between these alternatives to justify high lactate production, we used murine 3T3L1 adipocytes exposed to varying glucose concentrations in the medium, under full oxygen availability, and determining how these conditions modulate fat deposition, lactate production and oxygen consumption.

Results

Substrate utilization during 3T3L1 adipocytes differentiation. Figure 1 shows the changes in cell volume and biomass (i.e. the sum of cells and debris produced during harvesting) accumulation in 3T3L1 cell cultures, from fibroblasts at confluence to mature adipocytes. Medium glucose (22 mM when fresh), decreased steadily with differentiation in spent media, in parallel to increasing lactate, which arrived at a plateau in the 25 mM range. These trends were maintained when the data were expressed as mean rates per cell. Proton release/leakage increased during differentiation with rates similar to those of glucose uptake.

Energy balance and glucose fate during the differentiation of 3T3L1 adipocytes. For the sake of calculations, we assumed that the cell components of a fibroblast and a mature adipocyte were similar, and the differences in size between them were largely due to accumulation of TAG.

The mean biomass of a confluent fibroblast culture was 1.27 µL/well, and that of mature adipocytes obtained from the same stock and number of fibroblasts was 3.59 µL/well at the end of the 9-day process. The difference in volume, assumed to be mainly fat, translated to about 2.07 mg/well, i.e. 2.3 µmol TAG, synthesized using 36 µmol glucose (for details see Supplemental Methods). On the other hand, the 9-day process of differentiation and growth of adipocytes consumed 196 ± 36 µmol glucose, producing 339 ± 4 µmol lactate. The amount of glucose converted to lactate was about 169 µmol, leaving only 27 µmol glucose for TAG synthesis and other uses, including oxidative energy production. Even assuming a wide margin of error in our assumptions, these values were in the same range than those calculated from biomass changes. These data suggest that practically all available glucose was used for lactate production and lipid synthesis.

In the process analyzed, 45% glucose (of the initial 22 mM) was taken up from the medium; about 80–86% of the incorporated glucose was converted to lactate, and 15–18% was used for TAG synthesis. From these data we can assume that ATP was mainly obtained from glycolysis: 339 µmol, 36 µmol were excess ATP produced from TAG synthesis, and the equivalent of 16 µmol was lost as H^+ leakage (assuming 3 protons per ATP). Thus, aerobic glucose oxidation was necessarily very low, since only the pyruvate dehydrogenase step in the lipogenic process was aerobic, and anaerobic pathways practically justified the entire glucose uptake. In consequence, 3T3L1 cells showed a markedly anaerobic metabolism under high glucose, even during differentiation and TAG storage.

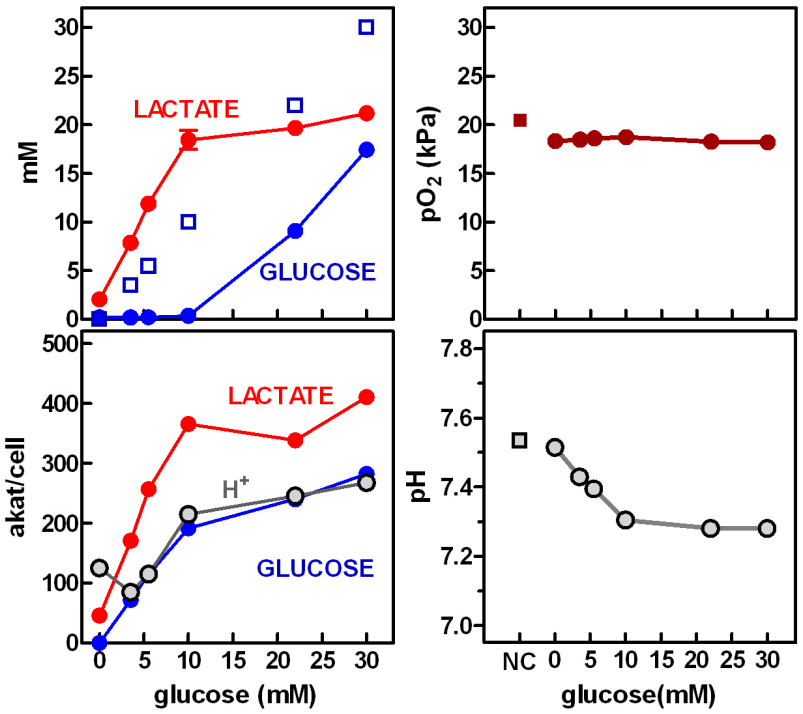

Figure 2 | Effects on glucose uptake, lactate efflux, pO_2 and pH of the concentration of glucose in the medium of 3T3L1 mature adipocytes. Left upper panel: medium glucose and lactate (mean ± SEM) after 3 days of incubation of the cells at the given glucose concentration. Blue squares represent the initial glucose concentration. The left bottom panel shows the same data presented as rates (attokatals per cell, mean values only); proton release into the medium has been also included (mean ± SEM).The right panels represent the pO_2 and pH *vs.* initial medium glucose concentration (mean ± SEM). NC correspond to a well incubated under the same conditions (i.e. [Glc] = 22 mM) but containing no cells.

Figure 2 presents the medium lactate and glucose concentrations after incubation of mature 3T3L1 cells (from days 6 to 9). Glucose levels were practically zero in the spent media from initial values of 0 to 10 mM, reaching up to 17 mM for the 22–30 mM range. The zero values observed below 10 mM suggest that total removal of glucose under these conditions could have gone beyond these values if more glucose were initially available. On the other hand, lactate levels increased up to 20 mM but then leveled off irrespective of glucose availability. The adjustment of medium concentrations to rates per cell repeated the same pattern. There was a significant release of protons, parallel to glucose uptake.

Effect of medium glucose concentration on adipocyte uptake of glucose and lactate production. No morphological differences between adipocytes exposed to different glucose concentrations were observed (Supplemental Figure 1) and no fibroblasts were observed in any glucose-concentration group. Biomass and cell size/counts were not significantly different either, but there were slight differences in total cell mass and biomass (Supplemental Figure 2). In our calculations, the changes in biomass were equalized by cell counts, and resulted in a net production (in 3 days) of −0.13 mg (at glucose 0 mM) to 0.34 mg (at glucose 22 mM). At concentrations of glucose 10–30 mM, the percentage of glucose uptake used for lipid synthesis was in the range of 11–12%, with smaller percentages for lower initial glucose levels (Supplemental Table 1). Lactate was produced (4.2 µmol) even at 0 mM glucose; it was probably formed from alanine or residual glucose from previous medium change. Glucose uptake (with respect to medium glucose) decreased from a maximal 94% at 3.5 mM to 42% at 30 mM. Conversion of glucose taken up to lactate decreased from 120% at 3.5 mM to 76% at 22 mM. The mean proportion of glucose conversion to lactate was 98% and the leakage of protons was equivalent to about 5% of the ATP obtained from lactate.

Figure 2 also presents the values of pH and pO_2 in the medium of 3T3L1 cells exposed to different glucose concentrations. The pO_2 of wells with no cells was 20.5 kPa, a figure close to that calculated from incubator atmosphere gas composition (20 kPa). The presence of cells resulted in a slight decrease of pO_2, in a range of 18.2 kPa to 18.7 kPa, with no differences between the groups, but all of them being lower than the no-cell control well ($p < 0.05$, Student's *t* test). The high pO_2 values showed that the cells were not under hypoxic conditions.

The medium pH in the no-cell control well was 7.54, and decreased in those with cells, the lowest value, 7.28 corresponding to the highest initial glucose concentrations ($p < 0.001$ for initial glucose; one way ANOVA). The acidification was due to proton leakage from the cells, proportional to glucose concentration.

Gene expression during the differentiation of 3T3L1 cells to adipocytes. Since the use of Transwells eliminated the presence of non-differentiated fibroblasts in wells containing only adipocytes[31], we were able to refer the gene expression data to cell numbers, since the semiquantitative method used for gene expression analysis allowed this type of comparisons[32]. The results were presented as mean number of copies of the corresponding mRNA per cell. This is only an approximation, but given the homogeneous origin of the samples, they allow comparisons of the expression data between different groups.

Figure 3 shows the expressions of a number of representative genes of glucose metabolism, lipid synthesis, handling and storage and a few regulatory genes controlling these processes or used as signals to other tissues. All genes studied showed a significant effect of differentiation/growth on their expressions, but followed different patterns. The number of copies for lactate dehydrogenase a (muscle type), and fatty acid transporter protein Ap2 were more than three orders of magnitude higher than those with the smallest number of copies: leptin and carnitine palmitoleoyl-transferase. Hexokinase

Table 1 | Lactate dehydrogenase activity and gene expressions in liver and adipose tissue of adult male Wistar rats

parameter	units	liver	subcutaneuos WAT	epididymal WAT
lactate dehydrogenase (EC 1.1.1.27)				
tissue activity	μkat/g protein	31.2 ± 1.5^{A}	3.11 ± 0.55^{B}	1.88 ± 0.14^{B}
Ldha expression	pmol/g protein	12890 ± 1150^{A}	1.51 ± 0.48^{B}	0.728 ± 0,051^{B}
Ldhb expression	pmol/g protein	5.85 ± 0.74^{A}	1.33 ± 0.40^{B}	0.678 ± 0.101^{B}
Ldha/Ldhb expression ratio		2203	1.13	1.07
expression of genes for enzymes controlling fatty acid synthesis/pyruvate oxidation				
Acc1 (acetyl-CoA carboxylase 1)	fmol/g protein	2360 ± 245^{A}	175 ± 63^{B}	109 ± 19^{B}
Fas (fatty acid synthase)	pmol/g protein	7.22 ± 0.70^{A}	10.84 ± 4.38^{AB}	1.24 ± 0.28^{B}
Pdk4 (pyruvate dehydrogenase kinase 4)	fmol/g protein	866 ± 105^{A}	174 ± 63^{B}	13 ± 4^{C}

Non-individual values are the mean ± sem of 6 different animals. Groups with different superscript letter are significantly different ($p < 0.05$, one-way ANOVA).

and pyruvate dehydrogenase kinase 4 showed a similar pattern: increased expression during the development period followed by a drop in the largest adipocytes. Preadipocyte factor 1, as expected, showed a reverse pattern, high on fibroblasts and lower in all adipocytes. The rest of genes studied followed a similar time-related pattern, increasing their expression during the different stages of differentiation from fibroblasts to a maximum in 9-day mature adipocytes.

Gene expression modulation during exposure to changing glucose concentration in the medium. In Figure 4, the effects of medium glucose on gene expression are shown. Here, the significance of differences between groups was limited to hexokinase, phophofructokinase (muscle type), lactate dehydrogenase a (muscle type), carnitine palmitoleoyl-transferase, hormone-sensitive lipase, adipose TAG lipase, PPARγ, 11β-hydroxysteroid dehydrogenase type 1 and leptin. Most patterns showed slight changes only, with lowest expression values at 30 mM glucose; the typical pattern, better exemplified by hexokinase showed a slight rise from 0 mM to 3.5 mM glucose followed by a progressive decrease in expression with increasing medium glucose. There was a lack of significant changes in all genes coding for enzymes implicated in lipid synthesis in spite of the actual increase in TAG synthesis (i.e. fat stores grew) in parallel to medium glucose. The expression of the main lactate dehydrogenase (muscle type) isoform decreased in spite of increasing lactate production with high medium glucose.

The ratio of transcripts per cell between total lactate dehydrogenase and muscle type enzyme gave a mean of 94.3 ± 0.3% of transcripts for muscle type enzyme, i.e. practically all (ratio in the range of 19/20). Thus, 3T3L1 cell lactate dehydrogenase belongs to the muscle type isozyme.

In vivo analysis of rat tissue lactate and lactate dehydrogenase. Table 1 shows the lactate dehydrogenase activity in the rat tissues tested, as well as the expressions of lactate dehydrogenases and a genes controlling fatty acid synthesis. Liver lactate dehydrogenase activity was one order of magnitude higher per g of protein than that of WAT. However, the differences in expression of the genes for this enzyme were much higher, between 3 and 4 orders of magnitude larger: i.e. WAT lactate dehydrogenase activity was related to a much lower amount of copies of both mRNA^{Ldha} and mRNA^{Ldhb} than liver in spite of the latter higher specific activity.

WAT locations showed similar expressions of both genes coding for lactate dehydrogenases, which suggests that in adult male rats half of the transcripts were of the muscle subtype and the other half of the heart isoform, whilst the liver was overwhelmingly of the muscle type as has been previously established[33]. All gene expressions investigated showed that subcutaneous WAT had higher expression levels than epididymalWAT, the differences being, however, not significant, in part because of high individual variation. The expression of *Acc1* and *Pdk4* were one order of magnitude lower in WAT than those of *Ldha* and *Ldhb*, but not than that of *Fas*, which also showed the highest variability.

Table 2 presents the plasma levels of lactate and glucose in blood plasma, and the concentrations of lactate in tissue (per g of tissue and as molality fraction), as well as the molality quotients between tissues and plasma. Glycemia was relatively high for normal rats (they were under isoflurane anesthesia, which increases glycemia, when killed), but was maintained within the range of normalcy for this stock. The levels of tissue lactate in liver (μmol/g) were four-fold higher than the circulating plasma levels, but those of WAT were lower. However, when only water space was taken into account (i.e. discarding the mass of TAG), the molality ratios of tissue lactate to plasma showed that in both WAT sites and liver, tissue lactate concentration was higher than in plasma.

Discussion

A key finding of this study is that lactate production by 3T3L1 adipocytes is not a consequence of hypoxia. Direct measurement of pO_2 showed that cultured cells had higher oxygen availability than that of blood plasma. Along the whole process of differentiation and growth, only a fraction of the widely available medium glucose was converted to TAG, whilst a larger proportion of the available glucose was converted to lactate through a fully anaerobic pathway.

Why was so much glucose metabolized anaerobically (i.e. wasted from the point of view of carbon or energy utilization) in the presence of sufficient oxygen to sustain a more efficient aerobic glucose oxidation? Did the cells show a Warburg effect[28,30]? It is plausible that a Warburg-like mechanism may suffice to cover the cell energy needs under conditions of rapid growth and abundance of energy substrates, since the ATP yield of glycolysis may be enough for rapid cell buildup, as in tumors[29]. However, the results we obtained do not support a Warburg-like effect for adipocytes, since the ability to use glucose through glycolysis to lactate as end-product was parallel to cell differentiation and lipid accrual. It may be expected to find a maximal Warburg effect at the earlier stages of differentiation, i.e. fibroblasts, but we observed just the reverse. In addition, we found no cell proliferation (cells' numbers did not increase; adipocytes only grew larger), another factor for active glycolysis in the presence of oxygen[30].

Lactate production in the presence of varying proportions of glucose suggests that the adipocyte is probably a "obligatory glycolytic" cell. In fact, mature adipocytes produced lactate even at glucose 0 mM (probably from alanine and/or remnants of previous medium). Glycolysis, apparently, took precedence upon lipid synthesis and storage (as shown by the different accrual of biomass). Medium glucose did not affect the expression of enzymes implied in the synthesis of fat, but modified those affecting its degradation and the incorporation of exogenous fatty acids. The strictest control was apparently directed, in fact to limit the entry of glucose into the cells (i.e. hexokinase[34]) and to lower the expression of lactic acid dehydrogenases, perhaps to regulate glucose wasting. Nevertheless, the

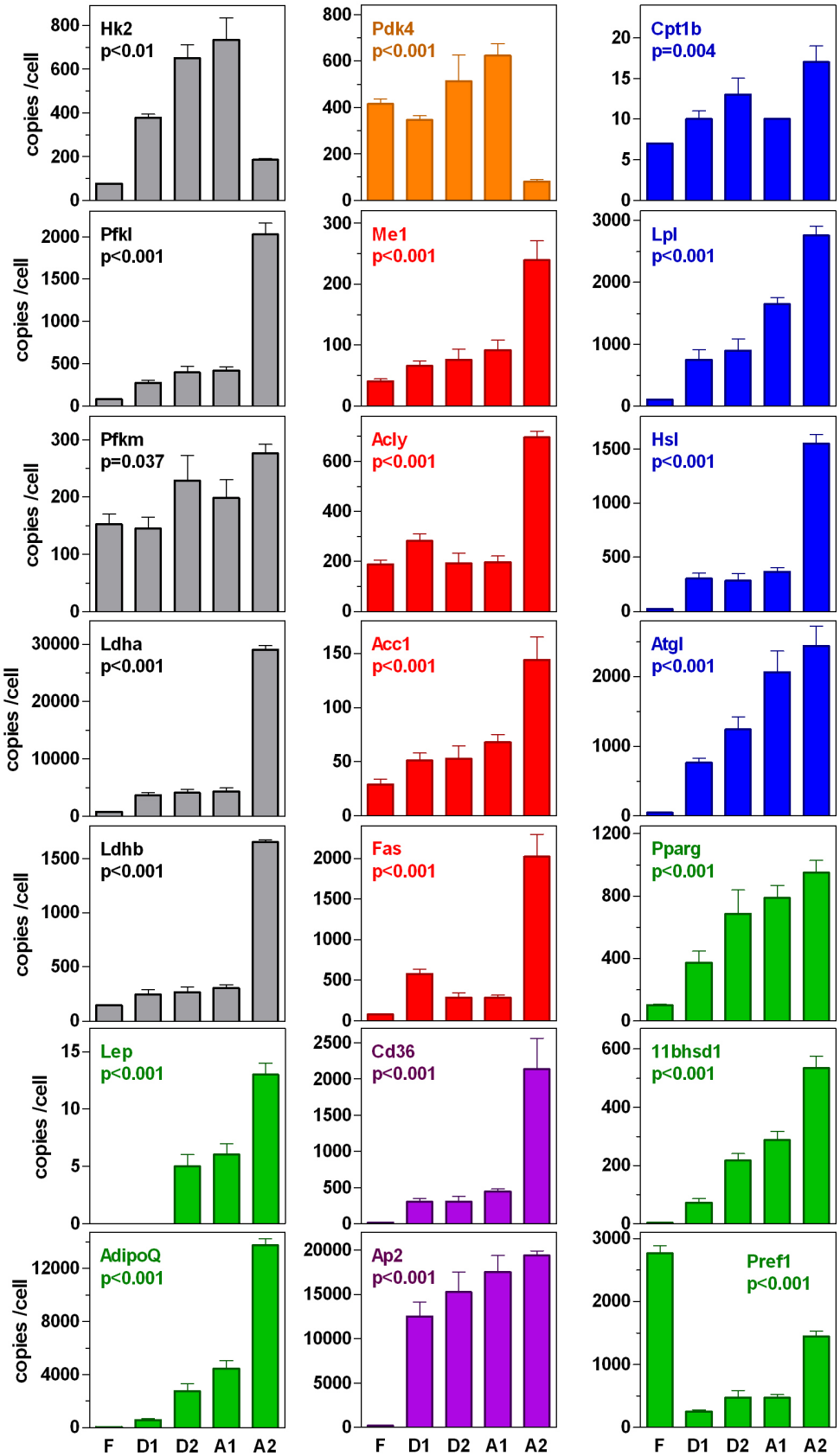

Figure 3 | Levels of expression of key genes in 3T3L1 cells during the differentiation process from fibroblasts (at confluence) to mature adipocytes. F = fibroblasts at confluence; D1 = end of the treatment with the first differentiation medium; D2 = end of the treatment with the second differentiation medium; A1 = mature adipocytes (day 6); A2 = mature adipocytes (day 9). The columns represent the mean (±sem) number of copies of the corresponding mRNA per cell at the different stages of differentiation. The statistical significance of changes along the process (one-way ANOVA) is given within each panel. Grey: carbohydrate catabolism pathways; Orange: 3C to 2C conversion; Red: lipogenesis; Blue: TAG catabolism; Purple: fatty acid transport; Green: regulatory agents.

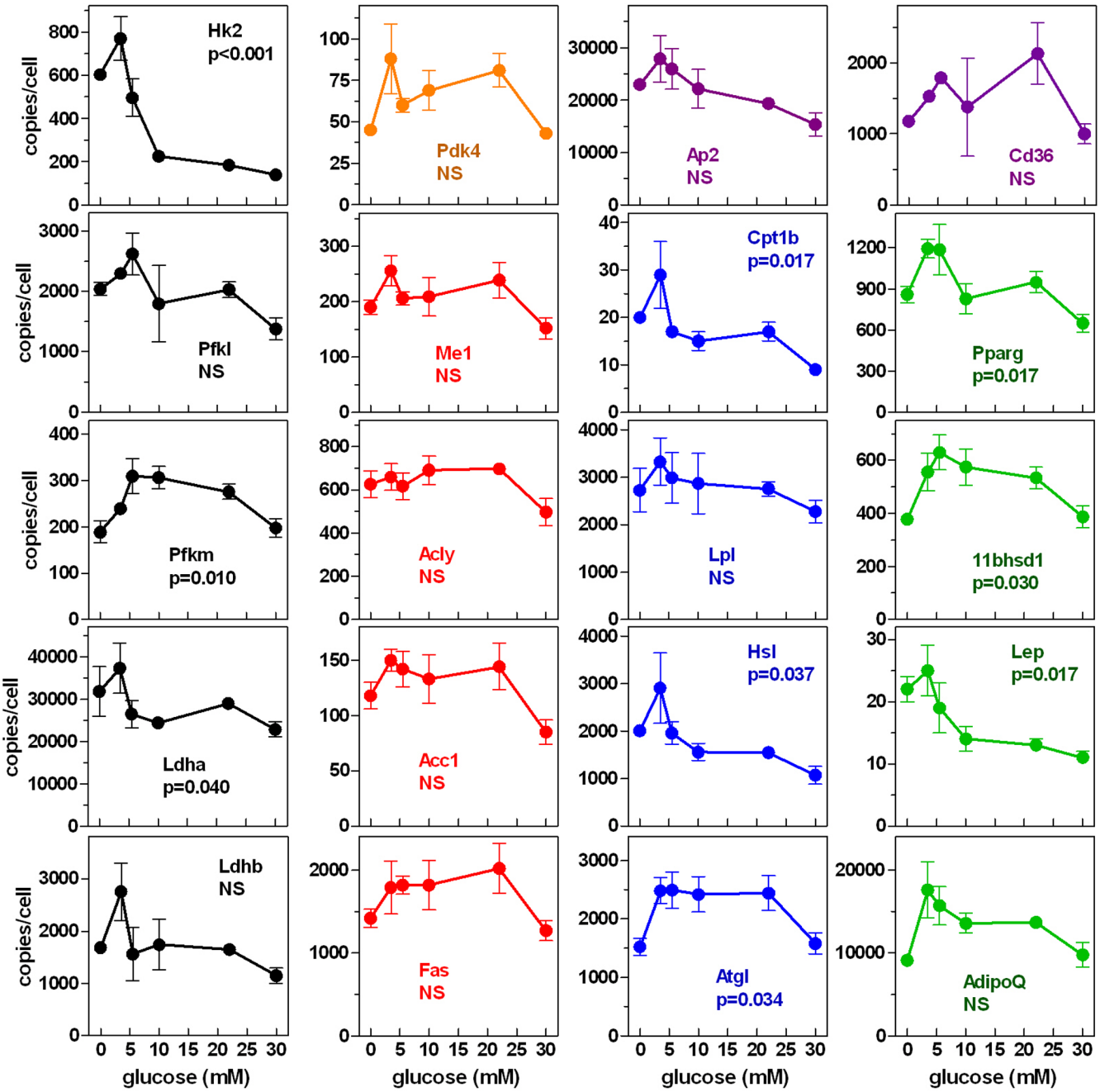

Figure 4 | Levels of expression of key genes in mature 3T3L1 adipocytes incubated during three days at different glucose concentrations in the medium. Points represent the mean (±sem) number of copies of the corresponding mRNA per cell. The statistical significance of the effect of medium glucose concentration (one-way ANOVA) is given within each panel. Grey: carbohydrate catabolism pathways; Orange: 3C to 2C conversion; Red: lipogenesis; Blue: TAG catabolism; Purple: fatty acid transport; Green: regulatory agents.

amount of glucose broken up to lactate was sustained at high rates even at the highest glucose concentrations.

Uncoupling of mitochondrial oxidative phosphorylation in 3T3L1 cells increases glycolysis to lactate at the expense of lipogenesis[35]. The sum of the largely anaerobic processes of synthesis of TAG and glycolysis to lactate accounted for practically all glucose. When the protons released (i.e. not used by the mitochondria for energy) were taken into account as their energy equivalent, the conclusion was that 3T3L1 cells had practically nil needs (and, consequently, consumption) of oxygen under the conditions tested.

The lack of changes in pO_2 with increasing medium glucose levels also hints at the lack of relationship between the abundance of the cells' main substrate and oxidative metabolism. The data we present here suggest that 3T3L1 adipocytes are essentially anaerobic even during lipogenesis and TAG storage. However, it must be taken into account that WAT contains other types of fully aerobic cells (stromal) in addition to adipocytes, and thus WAT as a whole may be more susceptible to hypoxia than its main constituent, adipocytes alone. Our results using 3T3L1 cells can be safely attributed solely to adipocytes[31].

Our *in vivo* data show that WAT lactate dehydrogenase activity was relatively high in comparison with other enzyme activities of the tissue. Lactate molality ratios *vs.* plasma were always positive, thus, rat WAT produced lactate under standard conditions, in agreement with the existence of lactate gradients in animal and human models[14,16]. Circulating lactate is increased in the immediate postprandial

Table 2 | Lactate concentrations in plasma, liver and adipose tissue of adult male Wistar rats

tissue lactate

parameter	units	liver	subcutaneous WAT	epididymal WAT	blood plasma
plasma glucose	mM				9.84 ± 0.42
tissue water content	g water/g tissue	0.77	0.36	0.17	0.91
tissue lactate concentration	µmol/g tissue (mM in plasma)	14.6 ± 0.75^{A}	2.08 ± 0.71^{BC}	1.68 ± 0.23^{B}	3.10 ± 0.29^{C}
	µmol/g water (molality)	19.0	5.8	10.1	3.4
tissue/plasma molality ratio		5.6	1.7	3.0	1.0

Non-individual values are the mean ± sem of 6 different animals. Groups with different superscript letter are significantly different ($p < 0.05$, one-way ANOVA).

state, rising later than glucose and insulin[36]. The process is quantitatively important, since, in insulin-resistant humans, WAT converts to lactate up to 2/3 of all glucose taken up[13]. The rapid conversion of glucose to lactate has been also observed *in vivo*, in human subcutaneous WAT[16,37], at rates that exceed the relatively low needs for energy of WAT itself. High liver lactate molality ratios reflect its role as lactate receptor in the Cori cycle, since lactate is a prime substrate for gluconeogenesis[15].

Adipocytes, by massively breaking up glucose to lactate (especially when WAT mass is large), lower glycemia, thus contributing to maintain glucose homeostasis. The process is mainly sustained by large adipocytes[9], thus we can assume that WAT glucose removal (and overall lactate production) are increased in obesity[38], in spite of locally reduced blood flow and access to substrates.

High glucose levels tend to decrease the relative ability of 3T3L1 cells to produce lactate from glucose (lower gene expressions); but, in absolute terms, this was not translated into decreased lactate production. We can speculate that the limit of glucose uptake and lactate production may, rather, depend on the ability to use the ATP generated, since the net ATP consumption of lipogenesis is small (Supplemental Figures 3 and 4), and its needs for adipocyte maintenance are limited.

From the data presented we can postulate an additional role for adipocytes in energy homoeostatic regulation: WAT helps decrease plasma glucose, especially under hyperglycemia, and thus indirectly improving insulin resistance[39]. As indicated above, WAT is the last dumping site for glucose under insulin resistance-induced hyperglycemia[27,40]. In WAT, excess glucose is used, in part, to build up TAG stores, but most of the glucose, unwanted elsewhere, is converted to lactate, which could be used as substrate by a number of tissues[41,42]. Most of circulating lactate, however, is taken up by the liver[43] and oxidized to pyruvate. Under conditions of excess glucose, in the liver, the gluconeogenic pathway remains inhibited[44], and the excess 3C is oxidized to acetyl-CoA via pyruvate dehydrogenase, followed by oxidation in the Krebs cycle (if not already saturated), or its utilization in other pathways. Since ketogenesis is also inhibited by glucose[45], practically the only path open is lipogenesis, fully operational for lactate in the liver[46]. Accumulation of newly formed lipid may hamper liver function (steatosis), but liver TAG may be exported (via lipoproteins) to other tissues, including WAT, which thus receives the "unwanted glucose carbon" as lipoprotein-carried TAG fatty acids, aggravating the WAT problem of TAG storage.

In the long term, the process outlined may help extend the damages caused by excess nutrients, but on the short term may help limit the effects of sustained glucose peaks, facilitate energy partition via distribution of 3C substrates and the centralization (and control) of fat synthesis in the liver rather than in disperse WAT sites. The process we postulate is a bidirectional transposition of the well known glucose-fatty acid (or Randall) cycle[47].

In conclusion, cultured adipocytes are largely anaerobic, and produce huge amounts of lactate from glucose in normoxic conditions. It is speculated that the massive production of lactate, directly related to glucose availability, is a process of defense of the adipocyte, exporting glucose carbon (and the problem) to the liver as lactate, but it may be also a mechanism of control of hyperglycemia. The *in vivo* data obtained from male rats agree with this interpretation.

Methods

Effects of differentiation of 3T3L1 cells on gene expression and substrate utilization. A batch of 3T3L1 fibroblasts was allowed to grow and differentiate under standard conditions, as described in the Supplemental Procedures, using Transwell™ inserts (Corning Life Sciences)[31]. Cells were harvested at 0, 2, 4, 6 and 9 days after the beginning of fibroblast differentiation (i.e., day 0 cultures contained only confluent fibroblasts, and days 6–9 only mature adipocytes). Cells were harvested, counted and their total RNA extracted using the GenElute™ (RTN10, RTN70 and RTN350, from Sigma-Aldrich) isolation procedure, following the instructions of the provider. RNA was used for the gene expression analysis. Media were used for the analysis of glucose, lactate and proton leakage (as described in the Supplemental Procedures).

Cultured 3T3L1 cells exposure to different medium glucose concentrations. Mature 3T3L1 adipocytes (i.e., on day 6 after fibroblast confluence as described above) were used for the analysis of the effect of medium glucose concentration. The medium was prepared omitting glucose, which was added to final concentrations of 0, 3.5, 5.5, 10, 22 or 30 mM. These media were used the last three days of incubation, substituting the standard 22 mM glucose medium. Spent media were used for the analysis of pH, glucose and lactate concentrations. The cells were harvested, counted and used for the extraction of total RNA for gene expression analysis.

pO_2 in the medium during incubation conditions. During the cells' exposure to different glucose concentrations, on day 9 (i.e., before harvesting), the medium pO_2 was measured using 1 mL syringes equilibrated at 37°C, which were filled with medium and resealed. Measurements of pH and pO_2 were done within 15 min, using an ABL-5 gas analyzer (Radiometer; Copenhagen Denmark). Control wells contained fresh medium and were incubated with no cells.

Analysis of gene expression in cultured 3T3L1 cells. Total RNA from harvested cells in different experiments was quantified using a ND-100 spectrophotometer (Nanodrop Technologies, Wilmington DE USA). RNA samples were reverse transcribed using the MMLV reverse transcriptase (Promega, Madison, WI USA) and oligo-dT primers.

Real-time PCR amplification was carried out using 10 µL amplification mixtures containing Power SYBR Green PCR Master Mix (Applied Biosystems, Foster City, CA USA), equivalent to 4 ng of reverse-transcribed RNA and 150 nM primers. Reactions were run on an ABI PRISM 7900 HT detection system (Applied Biosystems) using a fluorescent threshold manually set to OD 0.150 for all runs. The primers used for the estimation of murine (3T3L1 cells) gene expression are presented in Supplemental Table 2.

A semiquantitative approach for the estimation of the concentration of specific gene mRNAs per cell or unit of tissue weight was used[32]. *Rpl32* was used as charge control gene. The data were presented as the number of transcript copies per cell, allowing for direct comparisons independently ofthe number of cells in a given well.

In vivo study. Animals and housing conditions. Nine week old male Wistar rats (Harlan Laboratories Models, Sant Feliu de Codines, Spain) were used. The rats (N = 6) were housed in two 3-rat cages, had free access to water and were kept in a controlled environment (lights on from 08:00 to 20:00; 21.5–22.5°C; 50–60% humidity), and were fed standard rat chow (2014, Harlan).

The rats were kept, handled and killed following the procedures specifically approved by the University of Barcelona Animal Welfare and Ethics Committee, in accordance with the Rules set by the European Union and the Governments of Spain and Catalonia.

The animals were killed by exsanguination through the aorta under isoflurane anesthesia; samples of liver and WAT at the inguinal subcutaneous and epididymal fat pads were sampled, frozen in liquid nitrogen, and stored at −80°C. Blood plasma was separated from (heparinized) blood and kept frozen at −80°C.

Tissue lactate. Frozen tissue samples were weighed and homogenized in about 20 volumes of chilled water: acetone, to a final proportion of 1 : 1.2[48]. The samples were centrifuged at 0°C for 20 min at 4000 × *g*. Supernatants were delipidated (when needed) with finely powdered solid MgO, and used for the measurement of lactate (in parallel to plasma glucose and lactate) using the same procedures described (Supplemental Procedures) for cultured cell media.

Tissue and plasma lactate concentrations were expressed in molar units per g of fresh tissue weight, but also, as an estimate, per g of tissue water (molality). Adipose tissues contain about 70–80% of fat, which reduces considerably their water (and lactate) space[49]. The tissue (and plasma) water (i.e., lactate space) was estimated as shown in Supplemental Table 3. Calculation of theoretical tissue lactate concentration in these volumes of water was used to estimate the mean tissue *vs.* plasma lactate molality concentration ratios.

Measurement of lactate dehydrogenase activity. Frozen samples of liver were homogenized using a tissue disruptor (IKA-T10 basic Ultra-Turrax, IKA, Stauffen Germany) in 10 volumes of chilled Krebs-Ringer bicarbonate solution, pH 7.8 containing 5 mM dithiothreitol, 0.5% bovine serum albumin, 1% dextran (MW 200,000), 0.1% Triton X-100, and 1 mM EDTA[50]. Adipose tissue samples were homogenized in the same way as liver, but the homogenates were left standing for 5 min at 4°C. Sediments and floating fat-cakes were discarded, and only the intermediate layer was pipetted for lactate dehydrogenase activity. Homogenate protein was also estimated[51], using homogenization medium for blanks.

Total lactate dehydrogenase (EC 1.1.1.27) activity was measured in liver and WAT homogenates, using a standard kinetic NADH-oxidation UV method[52] to determine V_i values. Activity was expressed as nkat/g of wet tissue and μkat/g protein.

Analysis of gene expression in rat liver and WAT. Tissue total RNA was extracted from frozen tissue samples (about 30 mg) using the GenElute™ procedure. Gene expression was estimated as described for cultured cells, using a different set of primers; the list is presented in Supplemental Table 2. The semiquantitative approach described above was used for the estimation of the number of specific mRNA copies for each gene per unit of tissue weight and per g of protein. The genes studied coded for lactic acid dehydrogenases (muscle and heart), two key enzymes of fatty acid synthesis: acetyl-CoA carboxylase and fatty acid synthetase; and pyruvate kinase 4, which controls the use of pyruvate for oxidation to Acetyl-CoA. The *Ppia* gene was used as control of charge.

Statistical analyses. Comparisons between groups were done using one-way ANOVA analyses and the Bonferroni post-hoc test with the Prism 5 (GraphPad Software, San Diego CA USA) graphics/statistics package. Analysis of correlations and curve fitting were done using the same program. The Student's *t* test was also used for comparison between isolated data groups.

1. Weber, G., Banerjee, G. & Ashmore, J. Activities of enzymes involved in glycolysis, glucogenesis and hexosemonophosphate shunt in rat adipose tissue. *Biochem. Biophys. Res. Commun.* **3**, 182–186 (1960).
2. Atsumi, T. *et al.* Expression of inducible 6-phosphofructo-2-kinase/fructose-2,6-bisphosphatase/PFKFB3 isoforms in adipocytes and their potential role in glycolytic regulation. *Diabetes* **54**, 3349–3357 (2005).
3. Acheson, K. J. *et al.* Glycogen storage capacity and de novo lipogenesis during massive carbohydrate overfeeding in man. *Am. J. Clin. Nutr.* **48**, 240–247 (1988).
4. Shadid, S., Koutsari, C. & Jensen, M. D. Direct free fatty acid uptake into human adipocytes in vivo. Relation to body fat distribution. *Diabetes* **56**, 1369–1375 (2007).
5. Lasunción, M. A. & Herrera, E. "In vitro" utilization of labelled esterified fatty acids and glyceride glycerol from triglyceride-rich lipoproteins in rat adipose tissue. *Horm. Metabol. Res.* **13**, 335–339 (1981).
6. Weinstock, P. H. *et al.* Lipoprotein lipase controls fatty acid entry into adipose tissue, but fat mass is preserved by endogenous synthesis in mice deficient in adipose tissue lipoprotein lipase. *Proc. Nat. Acad. Sci. USA* **94**, 10261–10266 (1997).
7. Thacker, S. V., Nickel, M. & DiGirolamo, M. Effects of food restriction on lactate production from glucose by rat adipocytes. *Am. J. Physiol.* **253**, E336–E342 (1977).
8. Jansson, P. A., Smith, U. & Lonnroth, P. Evidence for lactate production by human adipose tissue in vivo. *Diabetologia* **33**, 253–256 (1990).
9. DiGirolamo, M., Newby, F. D. & Lovejoy, J. Lactate production in adipose tissue: a regulated function with extra-adipose implications. *FASEB J.* **6**, 2405–2412 (1992).
10. Newby, F. D., Wilson, L. K., Thacker, S. V. & DiGirolamo, M. Adipocyte lactate production remains elevated during refeeding after fasting. *Am. J. Physiol.* **259**, E865–E871 (1990).
11. King, J. L. & DiGirolamo, M. Lactate production from glucose and response to insulin in perifused adipocytes from mesenteric and epididymal regions of lean and obese rats. *Obesity Res.* **6**, 69–75 (2001).
12. Nellemann, B., Gormsen, L. C., Sørensen, L. P., Christiansen, J. S. & Nielsen, S. Impaired insulin-mediated antilipolysis and lactate release in adipose tissue of upper-body obese women. *Obesity* **20**, 57–64 (2012).
13. Kashivagi, A. *et al.* In vitro insulin resistance of human adipocytes isolated from subjects with noninsulin-dependent diabetes mellitus. *J. Clin. Invest.* **72**, 1246–1254 (1983).
14. Newby, F. D., Sykes, M. N. & DiGirolamo, M. Regional differences in adipocyte lactate production from glucose. *Am. J. Physiol.* **255**, E716–E722 (1988).
15. Cori, C. F. The glucose-lactic acid cycle and gluconeogenesis. *Curr. Top. Cell. Regulat.* **18**, 377–387 (1981).
16. Hagström, E., Arner, P., Ungerstedt, U. & Bolinder, J. Subcutaneous adipose tissue: a source of lactate production after glucose ingestion in humans. *Am. J. Physiol.* **258**, E888–E893 (1990).
17. Sahlin, K. Lactate formation and tissue hypoxia. *J. Appl. Physiol.* **67**, 2640 (1989).
18. Sestoft, L., Bartels, P. D. & Folke, M. Pathophysiology of metabolic acidosis: effects of low pH on the hepatic uptake of lactate, pyruvate and alanine. *Clin. Physiol.* **2**, 51–58 (1982).
19. Soares, A. F. *et al.* Effects of oxidative stress on adiponectin secretion and lactate production in 3T3-L1 adipocytes. *Free Radic. Biol. Med.* **38**, 882–889 (2005).
20. Carrière, A. *et al.* Mitochondrial reactive oxygen species control the transcription factor CHOP-10/GADD153 and adipocyte differentiation - A mechanism for hypoxia-dependent effect. *J. Biol. Chem.* **279**, 40462–40469 (2004).
21. del Rio, R., Moya, E. A. & Iturriaga, R. Differential expression of pro-inflammatory cytokines, endothelin-1 and nitric oxide synthases in the rat carotid body exposed to intermittent hypoxia. *Brain Res.* **1395**, 74–85 (2011).
22. Hosogai, N. *et al.* Adipose tissue hypoxia in obesity and its impact on adipocytokine dysregulation. *Diabetes* **56**, 901–911 (2007).
23. Goossens, G. H. *et al.* Increased adipose tissue oxygen tension in obese compared with lean men is accompanied by insulin resistance, impaired adipose tissue capillarization, and inflammation. *Circulation* **124**, 67–76 (2011).
24. Hodson, L., Humphreys, S. M., Karpe, F. & Frayn, K. N. Metabolic signatures of human adipose tissue hypoxia in obesity. *Diabetes* **62**, 1417–1425 (2013).
25. McQuaid, S. E. *et al.* Downregulation of adipose tissue fatty acid trafficking in obesity. A driver for ectopic fat deposition? *Diabetes* **60**, 47–55 (2011).
26. Bohr, C., Hasselbalch, K. & Krogh, A. Über einen in biologischer Beziehung wichtigen Einfluss, den die Kohlensäurespannung des Blutes auf dessen Sauerstoffbindung übt. *Scand. Arch. Physiol.* **16**, 402–412 (1904).
27. Alemany, M. Regulation of adipose tissue energy availability through blood flow control in the metabolic syndrome. *Free Radic. Biol. Med.* **52**, 2108–2119 (2012).
28. Warburg, O. On the origin of cancer cells. *Science* **132**, 309–314 (1956).
29. López-Lázaro, M. The Warburg effect: Why and how do cancer cells activate glycolysis in the presence of oxygen? *Anti-Cancer Ag. Med. Chem.* **8**, 305–312 (2008).
30. van der Heiden, M. G., Cantley, L. C. & Thompson, C. B. Understanding the Warburg effect: The metabolic requirements of cell proliferation. *Science* **324**, 1029–1033 (2009).
31. Sabater, D., Fernández-López, J. A., Remesar, X. & Alemany, M. The use of Transwells™ improves the rates of differentiation and growth of cultured 3T3L1 cells. *Anal. Bioanal. Chem.* **405**, 5605–5610 (2013).
32. Romero, M. M., Grasa, M. M., Esteve, M., Fernández-López, J. A. & Alemany, M. Semiquantitative RT -PCR measurement of gene expression in rat tissues including a correction for varying cell size and number. *Nutr. Metab.* **4**, 26 (2007).
33. Everse, J. & Kaplan, N. O. Lactate dehydrogenases: structure and function. *Adv. Enzymol. Rel. Ar. Mol. Biol* **37**, 61–133 (1973).
34. DiPietro, D. L. Hexokinase of white adipose tissue. *Biochim. Biophys. Acta* **67**, 305–312 (1963).
35. Si, Y. G., Shi, H. & Lee, K. B. Metabolic flux analysis of mitochondrial uncoupling in 3T3-L1 adipocytes. *PLoS One* **4**, e7000 (2009).
36. Lovejoy, J., Mellen, B. & DiGirolamo, M. Lactate generation following glucose ingestion. Relation to obesity, carbohydrate tolerance and insulin sensitivity. *Int. J. Obesity* **14**, 843–855 (1990).
37. van der Merwe, M. T. *et al.* Lactate and glycerol release from subcutaneous adipose tissue in black and white lean men. *J. Clin. Endocrinol. Metab.* **84**, 2888–2895 (1999).
38. Mårin, P., Rebuffé-Scrive, M., Smith, U. & Björntorp, P. Glucose uptake in human adipose tissue. *Metabolism* **36**, 1154–1160 (1987).
39. Muñoz, S. *et al.* Chronically increased glucose uptake by adipose tissue leads to lactate production and improved insulin sensitivity rather than obesity in the mouse. *Diabetologia* **53**, 2417–2430 (2010).
40. Alemany, M. The defense of adipose tissue against excess substrate-induced hyperthrophia: Immune system cell infiltration and arrested metabolic activity. *J. Clin. Endocrinol. Metab.* **96**, 66–68 (2011).
41. Granata, A. L., Midrio, M. & Corsi, A. Lactate oxidation by bkeletal muscle during sustained contraction in vivo. *Pflügers Arch. Eur. J. Physiol.* **366**, 247–250 (1976).
42. Lopaschuk, G. D., Collins-Nakai, R. L. & Itoi, T. Developmental changes in energy substrate use by the heart. *Cardiovasc. Res.* **26**, 1172–1180 (1992).
43. Radziuk, J. & Pye, S. Hepatic glucose uptake, gluconeogenesis and the regulation of glycogen synthesis. *Diabet. Metab. Res. Rev.* **17**, 250–272 (2001).
44. Rognstad, R. Control of lactate gluconeogenesis by glucose in rat hepatocytes. *Arch. Biochem. Biophys.* **217**, 498–502 (1982).
45. Edson, N. L. Ketogenesis-antiketogenesis. Substrate competition in liver. *Biochem. J.* **30**, 1862–1869 (1936).
46. O'Hea, E. K. & Leveille, G. A. Significance of adipose tissue and liver as sites of fatty acid synthesis in the pig and the efficiency of utilization of various substrates for lipogenesis. *J. Nutr.* **99**, 338–344 (2013).

47. Randle, P. J., Garland, P. B., Hales, C. N. & Newsholme, E. A. The glucose fatty-acid cycle: its role in insulin sensitivity and the metabolc disturbances of diabetes mellitus. *Lancet* **281**, 785–789 (1963).
48. Soley, M. & Alemany, M. A rapid method for the estimation of amino acid concentration in liver tissue. *J. Biochem. Biophys. Meth.* **2**, 207–211 (1980).
49. Robert, M. & Alemany, M. Water compartments in the tissues of pentobarbital anesthetized rats. *IRCS Med. Sci.* **9**, 236–237 (1981).
50. Remesar, X., Arola, L., Palou, A. & Alemany, M. Arginase activity in the organs of fed and 24-hours fasted rats. *Horm. Metabol. Res.* **12**, 281–282 (1980).
51. Wang, C. S. & Smith, R. L. Lowry determination of protein in the presence of Tritonx X-100. *Anal. Biochem.* **63**, 414–417 (1975).
52. Bergmeyer, H. U. & Bernt, E. Lactate dehydrogenase UV assay with pyruvate and NADPH (eds. Bergmeyer, H. U. & Bernt, E.) 7–75 (Verlag Chemie, Weinheim, 1974).

Acknowledgments

Thanks are given to Dr. M. Riera, from the Department of Physiology, Faculty of Biology, University of Barcelona, for his help and guidance in the sampling, calibration and measuring of oxygen partial pressure in cell cultures. This study was financed in part by grants SAF2009-11739, AGL2011-23635, and SAF2012-34895, of the Plan Nacional de Investigación of the Government of Spain. CIBER Obesity and Nutrition (an initiative of the Institute of Health Carlos III of the Government of Spain) paid the salary of M.M. Romero, S. Arriarán was recipient of a pre-doctoral grant from the Government of Catalonia. Dr. D. Sabater and S. Agnelli worked *pro bono* for most of the study.

Author contributions

D.S. did all work on cell cultures, S.Ar. and S.Ag. did the in vivo studies including gene expression; M.M.R. analyzed cultured cells gene expressions; X.R. and J.A.F.L. carried out the analyses of media and did the statistics; M.A. did the experimental design and wrote the draft. All Authors participated in the discussion of the results and in the final redaction.

Additional information

Supplementary information accompanies this paper at http://www.nature.com/scientificreports

Competing financial interests: The authors declare no competing financial interests.

How to cite this article: Sabater, D. *et al.* Cultured 3T3L1 adipocytes dispose of excess medium glucose as lactate under abundant oxygen availability. *Sci. Rep.* **4**, 3663; DOI:10.1038/srep03663 (2014).

SUPPLEMENTAL MATERIALS

Cultured 3T3L1 adipocytes dispose of excess medium glucose as lactate under abundant oxygen availability

David **Sabater**, Sofía **Arriarán**, María del Mar **Romero**, Silvia **Agnelli**, Xavier **Remesar**, José Antonio **Fernández-López**, and Marià **Alemany**

SUPPLEMENTAL METHODS

Cells and transwell cell culture conditions

3T3L1 cells (ATCC-CL-173) were obtained from ATCC (Manassas, VA USA), and kept under liquid nitrogen; they were used at a passage not higher than 6. The cells were cultured in 6-well plates (Costar 3506, Corning Life Sciences, Corning, NY USA) with 24 mm polyester membrane Transwell inserts (Corning Life Sciences) under standard conditions as previously described [1], using DMEM-GlutaMAX-I (Gibco Life Technologies, Roche Diagnostics, Indianapolis, IN USA) supplemented with 10% newborn calf serum (NBS; Gibco Life Technologies), 25 mM Hepes, 100 U/mL penicillin and 100 mg/L streptomycin (all from Sigma-Aldrich, St Louis MO USA). Two days post-confluence, the cells were differentiated to adipocytes using the same medium containing 10% fetal bovine serum instead of NBS (basal medium), supplemented with 5 mg/L insulin, 0,25 μM dexamethasone and 0,5 mM IBMX (all from Sigma-Aldrich) [2]. After two days this medium was switched to one supplemented only with insulin, and two more days later the cells were kept in the basal medium with no added hormones. The basal medium contained 3.5 mM L-alanyl-L-glutamine and 22 mM glucose as N and energy substrates, and was changed every 2 days for up to 1 week. Under the conditions used, pH was maintained in all cases between 7.4 and 7.8. The cells were incubated in an oven at 37 ºC, ventilated with air supplemented with 5 % CO_2 which gave a theoretical pO_2 of 20 kPa (i.e. 0.2 mM dissolved O_2, almost twice the oxygen carried by blood plasma: 0.13 mM [3]. The pCO_2 was 5 kPa, corresponding to 1.7 mM dissolved CO_2 (values calculated at 25ºC, pH7.5) [4].

At the end of the experimental process, the spent medium was removed and the cells were harvested using trypsin (Sigma-Aldrich) and mechanical separation, following the protocol for trypsinization in transwell inserts established by the provider (Corning Life Sciences). Under these conditions, the cultures contained only plurivacuolar adipocytes, with nil presence of fibroblasts [1] (Supplemental Figure 1).

Spent incubation media were immediately frozen until used for the analysis of glucose (kit 11504, Biosystems, Barcelona Spain) and L-lactate (kit 1001330 Spinreact, Sant Esteve d'en Bas, Spain) using standard enzymatic methods.

All inorganic products and solvents were purchased from Panreac (Castellar del Vallès, Spain) and biochemicals from Sigma-Aldrich unless otherwise indicated.

Cultured cell counting and size estimation

Harvested cells were suspended in fresh medium and then their number and size distribution were measured with a portable cell counter, Scepter™ Handheld Automated Cell Counter (PHCC20060 Scepter, Merck Millipore, Billerica, MA USA). The settings of the instrument were adjusted for adipocyte size [1]. The total volume of particles was considered "total biomass", whilst that of particles within the 18-24 μm diameter range were

considered adipocytes [5] and their total number and volume ("cell volume") as well as mean cell volume were calculated from the Scepter count data (Supplemental Figure 2).

Measurement of medium pH and cell proton release/leakage

Direct pH measurements (using a standard pH meter) of the medium in wells containing cells were not different from those of spent medium just drained from the cells. A more precise measurement of spent medium pH was done by measuring the OD ratio of the medium at both 420 nm and 560 nm. Supplemental Figure 5(A) shows the visible light spectrum of the medium used (basically that of phenol red it contains). A shift in the height of the peaks corresponds to a change in the protonated *vs.* unprotonated form of the indicator, which allows the estimation of $[H^+]$ in the medium; Supplemental Figure 5(B) also shows the relationship between the 420 nm/560 nm OD ratios variations with pH.

Since the medium is a complex buffer system, the direct estimation of pH does not corresponds directly to the amount of protons released by the cells to the medium, and cannot be directly calculated because of the interaction of proteins and superimposing buffers (including the phenol red indicator itself). In order to measure the effect of proton release upon the medium pH, fresh medium was titrated using 0.1 N HCl (actually 0.092 N after titration against a base) under continuous pH measurement. Since the addition of HCl altered the final volume, the pH was calculated in reference to the initial volume by expressing pH as $[H^+]$ and calculating the total protons' concentration in the medium. The titration curve for medium pH *vs.* added H^+ is shown in Supplemental Figure 5(C). This curve allowed us to estimate the net emission of protons by the cells to the medium from the measurement of the spent medium pH.

Estimation of the glucose energy partition between oxidative and anaerobic pathways during 3T3L1 cell differentiation

In the differentiation experiment, calculations for 3T3L1 cells were referred to one cell in order to standardize the calculations obtained in different experiments and conditions. The main energy inputs to the system are the biomass of fibroblasts and the glucose drawn from the medium (i.e. initial glucose in fresh medium minus that found in spent medium). N metabolism has been left out of the equation because of difficulties in estimating total N in both cells and medium: the large amount of serum calf protein completely obscured any small change in this parameter; in addition, most "energy" in fibroblasts was protein, with almost nil triacylglycerols; in adipocytes, protein content is low (perhaps comparable to that of their fibroblast ancestors), but they accrue a high amount of fat. In addition, there are considerable technical difficulties in accurately measuring the actual fat content of cultured 3T3L1 cells, i.e. with the degree of precision needed for calculations.

Since mature adipocytes grew from non-fat storing fibroblasts we can safely assume that all their triacylglycerol stores were synthesized, during differentiation, from the glucose present in the medium. We calculated the new production of fat assuming (as an approximation) that the content of TAG in fibroblasts was negligible, thus the difference in total "biomass" between an adipocyte culture compared with an analogous fibroblast culture (with closely similar cell numbers) at confluence would give us an approximate value for net lipid (essentially TAG) synthesis during the whole process.

The energy outputs of cultured cells were essentially two: CO_2 from the oxidation of glucose, used for energy and the buildup of triacylglycerol reserves, as well as lactate, released in large amounts into the medium. As shown in

Supplemental Figure 3, the amount of glucose needed to synthesize 1 mmol of triacylglycerol [887 mg for *bis*-stearoyl-oleoyl-glycerol] under fully aerobic conditions are about 15.75 mmol glucose..

Cell lipid density was assumed to be 0.89 g/ml (i.e the mean of triolein, 0.915 g/ml, and tripalmitin, 0.873 g/mL), thus the volume of 1 mmol triacylglycerol corresponds to 997 μL. Since we know the total number of cells in the medium, and the total amount of glucose spent by the cells for purposes other than lactate synthesis, we can estimate the proportion of glucose used for triacylglycerol accrual to the mature adipocyte stage. Production of lactate from glucose yields only 2 ATP per mole of glucose (Supplemental Figure 4).

Supplemental Methods Reference List

1. Sabater,D., Fernández-López,J.A., Remesar,X., & Alemany,M. The use of Transwells™ improves the rates of differentiation and growth of cultured 3T3L1 cells. *Anal. Bioanal. Chem.* **405**, 5605-5610 (2013).

2. Janssen,O.E. & Hilz,H. Differentiation of 3T3-L1 pre-adipocytes induced by inhibitors of poly(ADP-ribose) polymerase and by related noninhibitory acids. *Eur. J. Biochem.* **180**, 595-602 (1989).

3. Pitman,R.N. Oxygen transport and exchange in the microcirculation. *Microcirculation* **12**, 59-70 (2005).

4. Carroll,J.J., Sluosky,J.D., & Mather,A.E. The solubility of carbon dioxide in water at low pressure. *J. Phys. Chem. Ref. Data* **20**, 1201-1209 (1991).

5. Saiki,A. *et al.* Suppression of lipoprotein lipase expression in 3T3-L1 cells by inhibition of adipogenic differentiation through activation of the renin-angiotensin system. *Metabolism Clin. Exp.* **57**, 1093-1100 (2008).

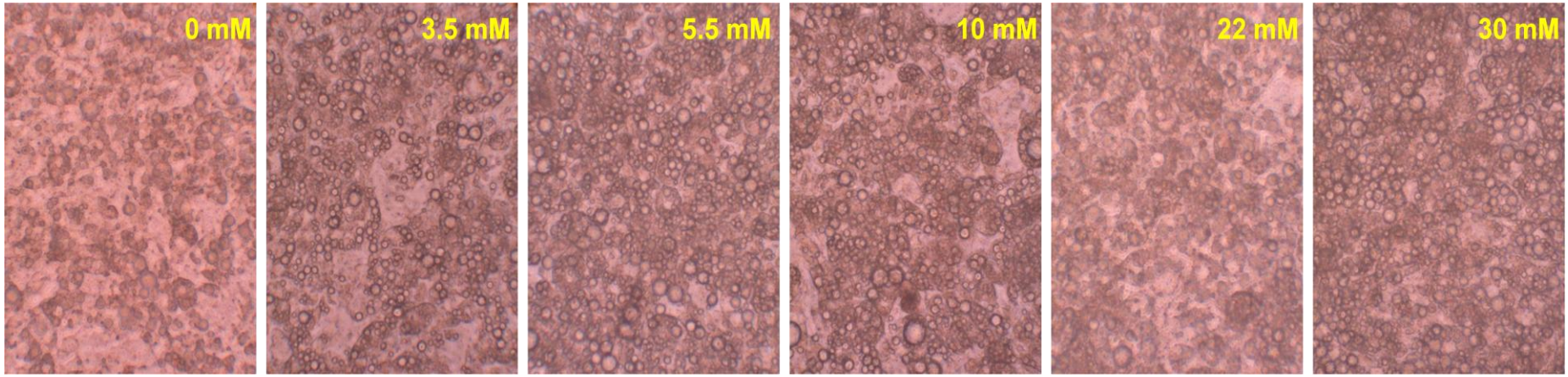

Supplemental Figure 1

Micrograph photographs of mature 3T3L1 cells after 3 days of incubation on a standard medium containing glucose at the concentrations shown in each photograph.

The width of each microphotograph corresponds to 160 μm

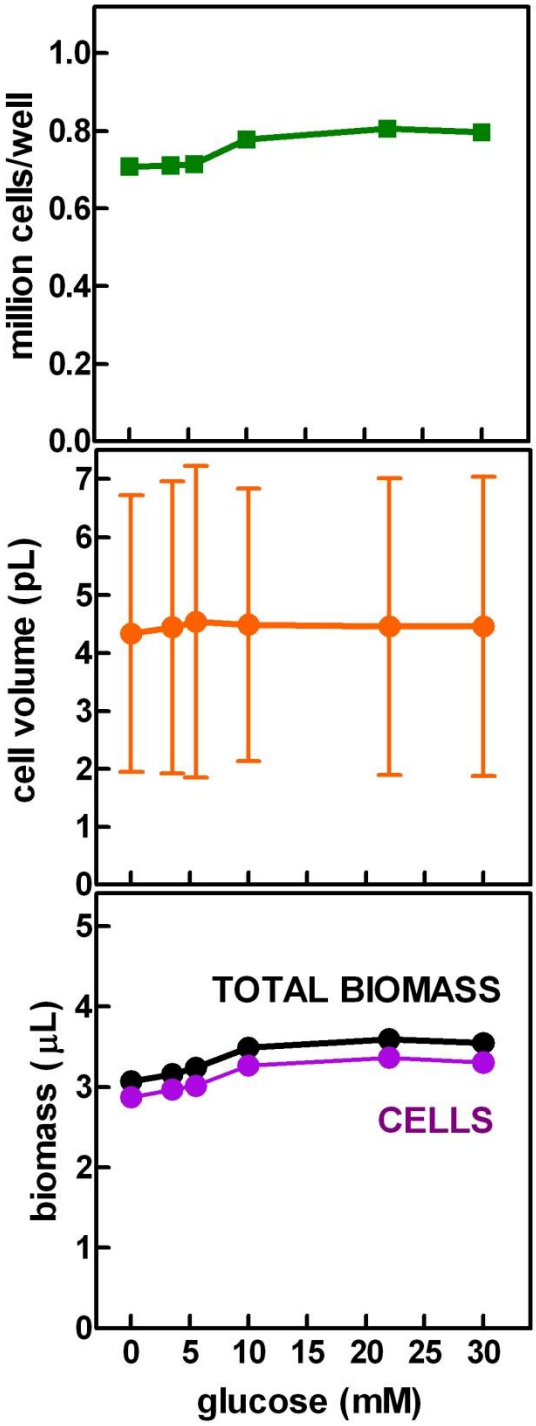

Supplemental Figure 2

Cell countings, cell volume and biomass of cultured mature 3T3L1 adipocytes exposed for 3 days to a medium with variable concentrations of glucose.

Cell counts and biomass data are presented as mean ± SEM, but cell volume (includes thousands of individual measurements) is shown as mean ± SD as a way to show a better representation of cell size variability.

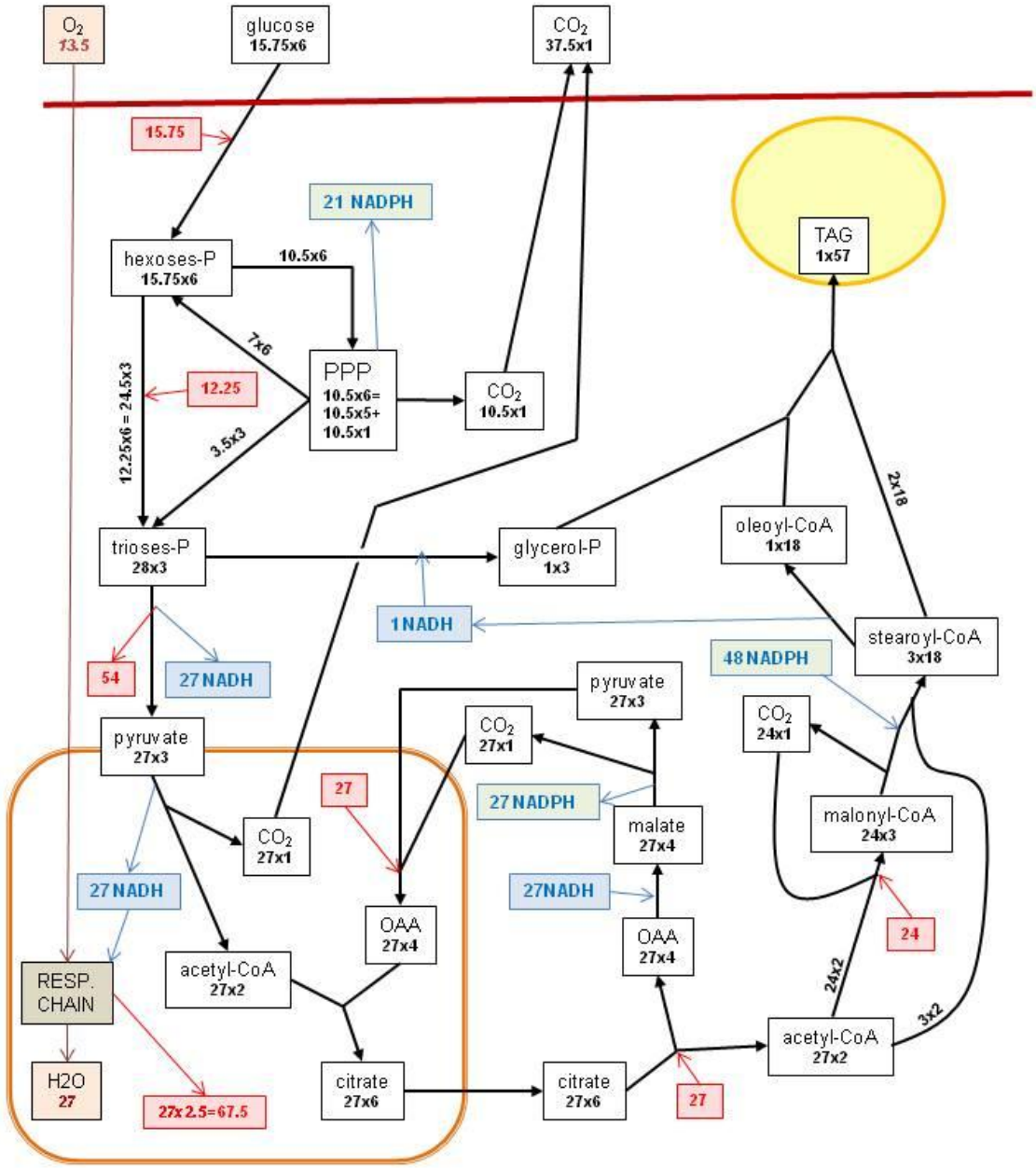

Supplemental Figure 3

Estimation of the needs of glucose, NADPH and ATP for the synthesis of 1 mol of TAG from glucose. The figures represent the flow of C (in black); the moles of ATP produced / consumed are shown in red, and the NADH and NADPH are shown in blue.

PPP = pentose-phosphate pathway

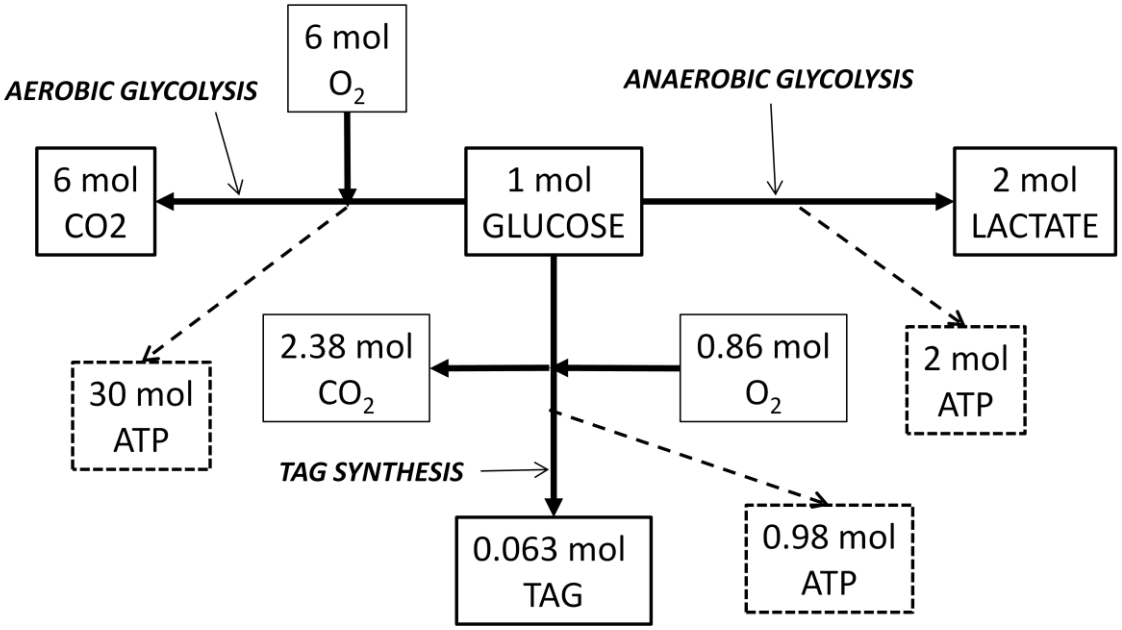

Supplemental Figure 4

Molar relationships between glucose, triacylglycerol and lactate depending on the pathway followed for glucose utilization

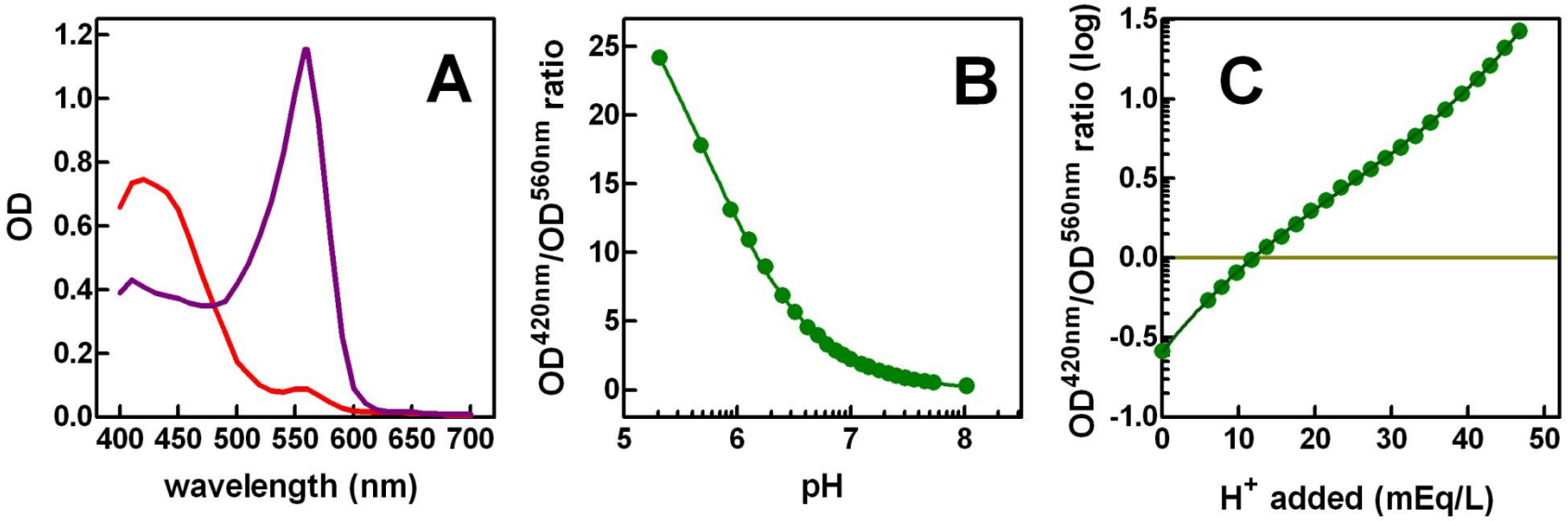

Supplemental Figure 5

A Spectral analysis of phenol red in cultured-cell incubation medium, shown at acidic pH (red line) and at neutral pH (purple line). The acidic form of the indicator has a maximal OD response at 420 nm and the neutral/basic one at 560 nm.

B relationship of the quotient of OD measured at 420 nm and 560 nm with the actual pH of the medium

C Effect of acidification of the cultured-cell incubation medium on pH or the quotient of OD at 420 nm/ OD at 560 nm.

Supplemental Table 1 Fate of the glucose taken up by mature 3T3L1 adipocytes from media with varying proportions of glucose

	units	Initial concentration of glucose in the medium (mM)					
		0	3.5	5.5	10	22	30
Glucose uptake from medium	µmol	-1.8	13.1	21.0	38.5	51.7	50.2
	% of medium	--	93.8	95.6	96.4	58.7	41.8
Glucose used for lipid synthesis	µmol	-2.24	-0.76	0.48	4.49	6.11	5.36
	% of intake	--	-5.81	2.26	11.6	11.8	10.7
Glucose used for lactate production	µmol	[4.17]	15.7	23.7	36.9	39.3	42.4
	% of intake	--	120	113	95.7	76.1	84.3
Glucose used for lactate+lipid	µmol	[1.93]	15.0	24.2	41.4	45.4	47.7
Glucose available for other uses	% of intake	[0.0]	-13.9	-15.2	-7.4	12.1	5.0

These values were calculated from the data shown in other graphs/tables, and are only a gross approximation to the actual data. Numbers between brackets indicate a non-glucose origin of the lactate found in the medium (i.e. alanine)

Supplemental Table 2 Primers used in the analysis of gene expression

Gene	Protein	Sequence 5’ → 3’	Sequence 3’ → 5’	size
Primers used for 3T3L1 cell gene expression analysis				
Hk2	hexokinase 2	CTCTCTCAACCCTGGCAAAC	GCACAATCTCGCCCAAGTA	68
Pfkl	phosphofructokinase, liver	CCAATGCTCCAGACTCAGC	AGATTCAGCCACCACTGCTC	130
Pfkm	phosphofructokinase, muscle	TGGTGCTGAGGAATGAGAAA	TCAAAGGGAGTTGGGCTTC	145
Ldha	Lactic acid dehydrogenase (muscle)	GCATCCCATTTCCACCAT	TCCGAGATTCCATTTTGTCC	96
Ldhb	Lactic acid dehydrogenase (heart)	GATTCACCCCGTGTCTACCA	AGCGACCTCATCGTCCTTC	136
Lep	leptin	AAGTCCAGGATGACACCAAAACC	GGTCCATCTTGGACAAACTCAGAA	121
AdipoQ	adiponectin	GCCGTTCTCTTCACCTACGA	ACTTGGTCTCCCACCTCCA	92
Pdk4	pyruvate dehydrogenase kinase 4	ACCGCATTTCTACTCGGATG	CTTGGGTTTCCCGTCTTTG	73
Me1	malic enzyme 1	TTCCTACGTGTTCCCTGGAG	GGCCTTCTTGCAGGTGTTTA	131
Acly	ATP citrate lyase	GATGAAGAAGGAGGGGAAGC	GGGAAGTGCTGTTTGACGA	111
Acc1	acetyl-CoA carboxylase α	GGAGCCAGAAGGGACAGTAGA	CAGCCAAGCGGATGTAAACT	92
Fas	fatty acid synthase	AGAGGCTTGTGCTGACTTCC	AATGTGCTTGGCTTGGTAGC	59
Cd36	fatty acid transporter (FTO)	AGAACAGCAGCAAAATCAAGG	ACAGTGAAGGCTCAAAGATGG	147
Ap2	fatty acid binding protein 4	AACACCGAGATTTCCTT	ACACATTCCACCACCAG	114

Cpt1b	carnitine palmitoyl-transferase 1b	CGCAGGAGGAAGGGTAGAGT	CCAGGGTCACAAAGAAAGCA	110
Lpl	lipoprotein lipase	GCCAAGAGAAGCAGCAAGAT	CCATCCTCAGTCCCAGAAAA	101
Hsl	hormone sentitive lipase	CTGCTTCTCCCTCTCGTCTG	CAAAATGGTCCTCTGCCTCT	108
Atgl	adipose tissue triacylglycerol lipase	CAAACAGGGCTACAGAGATGG	AAGGGTTGGGTTGGTTCAGT	68
Pparg	PPARγ	GCAGGAGCAGAGCAAAGAGG	CGAAACTGGCACCCTTGA	54
11bhsd1	11β-hydroxysteroid dehydrogenase 1	GGACGTATTGTGACCGTTG	GGTTCACATTAGTCACTGCAT	77
Pref-1	Pref-1 differentiation factor	TGGAACTTGCGTGGACCT	TGGCAGGGAGAACCATTGA	117
Rpl32	ribosomal protein L32 (housekeeping gene)	CTGGAGGTGCTGCTGATGT	GGGATTGGTGACTCTGATGG	123
Primers used for rat gene analysis				
Gene	Protein	Sequence 5’ → 3’	Sequence 3’ → 5’	size
Acc1	Acetyl-CoA carboxylase 1	AGGAAGATGGTGTCCGCTCTG	GGGGAGATGTGCTGGGTCAT	145
Ldha	Lactic acid dehydrogenase (muscle)	CACTGGGTTTGAGACGATGA	GTCAGCAAGAGGGAGAGAGC	125
Ldhb	Lactic acid dehydrogenase (heart)	CCAGGAACTGAACCCAGAGA	TCATAGGCACTGTCCACCAC	131
Fas	Fatty acid synthase	CTTGGGTGCCGATTACAACC	GCCCTCCCGTACACTCACTC	163
Pdk4	Pyruvate dehydrogenase kinase 4	GTCAGGCTATGGGACAGATGC	TTGGGATACACCAGTCATCAGC	137
Ppia	Cyclophilin A (housekeeping gene)	CTGAGCACTGGGGAGAAAGGA	GAAGTCACCACCCTGGCACA	87

Supplemental Table 3 Estimation of tissue water in plasma, liver and adipose tissues of adult male Wistar rats

tissue composition (in g/g tissue)				
parameter	liver	subcutaneous WAT	epididymal WAT	blood plasma
tissue lipid	0.041	0.576	0.809	0.011
tissue protein	0.181	0.063	0.050	0.075
tissue water	0.768	0.361	0.164	0.914

Tissue protein data were the same used for estimation of enzyme and lactate tissue concentrations. Lipid data are unpublished results obtained from animals of the same stock, age and sex than those used in this experiment. Tissue water is only an approximate value of the “lactate space” in the tissue.